

Research Journal of Pharmaceutical, Biological and Chemical Sciences

Corrosion protection of mild steel in hydrochloric acid solutions in presence of 5-(Benzyloxy)indole – Monte Carlo simulation, weight loss and electrochemical studies.

B. El Makrini¹, K. Toumiat², H. Lgaz^{3,4}, R. Salghi^{4*}, S. Jodeh⁵, G. Hanbali⁵, M. Belkhaouda², and M. Zougagh^{6,7}

¹Laboratory of Applied Chemistry and Environment, ENSA, Université Ibn Zohr, Agadir, Morocco.

²Department of Materials Sciences, Laghouat University, PO Box 37, 03000, Laghouat, Algeria.

³Laboratory separation processes, Faculty of Science, University Ibn Tofail PO Box 242, Kenitra, Morocco.

⁴Laboratory of Applied Chemistry and Environment, ENSA, Ibn Zohr University, PO Box 1136, 80000 Agadir, Morocco.

⁵Department of Chemistry, An-Najah National University, P. O. Box 7, Nablus, Palestine.

⁶Regional Institute for Applied Chemistry Research, IRICA, Ciudad Real, Spain.

⁷Albacete Science and Technology Park, E-02006, Albacete, Spain.

ABSTRACT

The inhibition effects of 5-(Benzyloxy)indole, noted 5BI on mild steel corrosion in 1.0 M HCl were studied with potentiodynamic polarization, electrochemical impedance spectroscopy techniques and weight loss studies. It was shown that 5BI act as good corrosion inhibitor for mild steel protection. The high inhibition efficiencies were attributed to the simple blocking effect by adsorption of inhibitor molecules on the steel surface. Molecular dynamics was carried out to establish mechanism of corrosion inhibition for mild steel with 5BI in acidic medium. The inhibition action of the compound was assumed to occur via adsorption on the steel surface through the active centers in the molecule following Langmuir isotherm model. The results indicated that the corrosion inhibition is due to the physical and chemical adsorption on the steel surface.

Keywords: Corrosion inhibition, Mild steel, *EIS*, Monte Carlo simulation, Indole

**Corresponding author*

INTRODUCTION

Mild steel is widely used in many industrial applications. In most industrial processes, the acidic solutions are commonly used for the pickling, industrial acid cleaning, acid descaling, oil well acidifying, etc. Unfortunately, iron and its alloys could corrode during these acidic applications particularly with the use of hydrochloric acid, which results in terrible waste of both resources and money[1–6]. The decreasing of corrosion rate of metals provides saving of resources and economical benefits during the industrial applications as well as increasing the lifetime of equipment and also decreasing the dissolution of toxic metals from the components into the environment[7–19]. Therefore, the prevention of metals used in industrial applications from corrosion is vital that must be dealt with. The use of organic molecules as corrosion inhibitor is one of the most practical methods for protecting metals against the corrosion and it is becoming increasingly popular[20–24]. The existing data show that organic inhibitors act by the adsorption and protect the metal by film formation. Organic compounds bearing heteroatoms with high electron density such as sulphur, nitrogen, oxygen or those containing multiple bonds which are considered as adsorption centers, are effective as corrosion inhibitors[25–27]. In the present investigation the corrosion inhibition performance of indole derivative (5BI) was studied by means of weight loss measurement, potentiodynamic polarization, electrochemical impedance spectroscopy (EIS) and Monte Carlo simulation studies.

MATERIALS AND METHODS

Electrodes, test solution and gravimetric measurements

Corrosion tests have been performed, using the gravimetric and electrochemical measurements, on electrodes cut from sheets of carbon steel with the chemical composition: 0.370 % C, 0.230 % Si, 0.680 % Mn, 0.016 % S, 0.077 % Cr, 0.011 % Ti, 0.059 % Ni, 0.009 % Co, 0.160 % Cu, and the remainder iron. The aggressive medium of molar hydrochloric acid used for all studies were prepared by dilution of analytical grade 37% HCl with double distilled water. The concentrations of 5BI used in this investigates were varied from 1.10^{-4} to 5.10^{-3} M. The inhibitor molecule used in this paper was purchased from Sigma–Aldrich and have the structure presented in Fig. 1. Gravimetric measurements were realized in a double walled glass cell equipped with a thermostat-cooling condenser. The carbon steel specimens used have a rectangular form with dimension of $2.5 \times 2.0 \times 0.2$ cm were abraded with a different grade of emery paper (320-800-1200) and then washed thoroughly with distilled water and acetone. After weighing accurately, the specimens were immersed in beakers which contained 100 ml acid solutions without and with various concentrations of 5BI at temperature equal to 303 K remained by a water thermostat for 6h as immersion time. The gravimetric tests were performed by triplicate at same conditions.

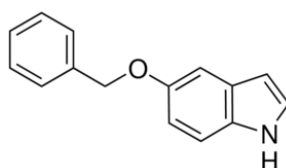
The corrosion rates (C_R) and the inhibition efficiency ($\eta_{wt}\%$) of carbon steel have been evaluated from mass loss measurement using the following equations:

$$C_R = \frac{w}{St} \quad (1)$$

$$\eta_{wt}\% = \frac{C_R^0 - C_R}{C_R^0} \times 100 \quad (2)$$

Where w is the average weight loss before and after exposure, respectively, S is the surface area of sample, t is the exposure time, C_R^0 and C_R is the corrosion rates of steel without and with the 5BI inhibitor, respectively.

Figure 1. Chemical structure of tested compound.



Electrochemical tests

The potentiodynamic polarization curves were conducted using an electrochemical measurement system PGZ 100 Potentiostat/Galvanostat controlled by a PC supported by the Voltmaster 4.0 Software. The electrochemical measurements were performed in a conventional three electrode glass cell with carbon steel as a working electrode, platinum as counter electrode (Pt) and a saturated calomel electrode used as a reference electrode. The working electrode surface was prepared as described above gravimetric section. Prior to each electrochemical test an immersion time of 30 min was given to allow the stabilization system at corrosion potential. The polarization curves were obtained by changing the electrode potential automatically from -800 to -200 mV/SCE at a scan rate of 1 mV s⁻¹. The temperature is thermostatically controlled at desired temperature ±1K. The percentage protection efficiency ($\eta_p\%$) is defined as:

$$\eta_{PDP}(\%) = \frac{I_{corr}^0 - I_{corr}}{I_{corr}^0} \times 100 \quad (3)$$

Where, I_{corr}^0 are corrosion current in the absence of inhibitor, I_{corr} are corrosion current in the presence of inhibitor.

Electrochemical impedance spectroscopy (EIS) measurements were carried out with same equipment used for potentiodynamic polarization study (Voltalab PGZ 100) at applied sinusoidal potential waves of 5mV amplitudes with frequencies ranging from 100 KHz to 10 mHz at corrosion potential. The impedance diagrams are given in the Nyquist representation. The charge transfer resistance (R_{ct}) was determined from Nyquist plots and double layer capacitance (C_{dl}) was calculated from CPE parameters of the equivalent circuit deduced using Zview software. In this case the percentage protection efficiency ($\eta_{EIS}\%$) is can be calculated by the value of the charge transfer resistance (Rct)

$$\eta_{EIS}(\%) = \frac{R_{ct} - R_{ct}^0}{R_{ct}} \times 100 \quad (4)$$

Where R_{ct}^0 and Rct were the polarization resistance of uninhibited and inhibited solutions, respectively.

Monte Carlo simulation study

The Monte Carlo (MC) search was adopted to compute the low configuration adsorption energy of the interactions of the 5BI on a clean iron surface. The Monte Carlo (MC) simulation was carried out using Materials Studio 7.0 software (Accelrys, Inc.) [28]. The Fe crystal was cleaved along the (1 1 0) plane, it is the most stable surface as reported in the literature. Then, the Fe (1 1 0) plane was enlarged to (10x10) supercell to provide a large surface for the interaction of the inhibitor. The simulation of the interaction between 5BI and the Fe: (1 1 0) surface was carried out in a simulation box (24.82 × 24.82 × 30.13 Å) with periodic boundary conditions, which modeled a representative part of the interface devoid of any arbitrary boundary effects. After that, a vacuum slab with 30 Å thickness was built above the Fe (1 1 0) plane. All simulations were implemented with the COMPASS force field to optimize the structures of all components of the system of interest. More simulation details on the methodology of Monte Carlo simulations can be found in previous publications [29–32].

RESULTS AND DISCUSSION

Gravimetric measurements

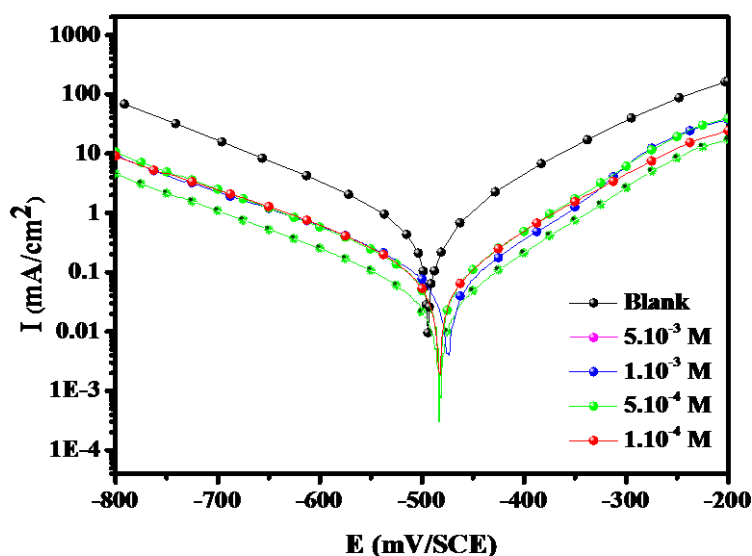
The corrosion rate of mild steel specimens after exposure to 1.0 M HCl solution with and without the addition of various concentrations of inhibitor was calculated in mg cm⁻² h⁻¹ and the data obtained are given in Table 1. The inhibition efficiencies ($I_E\%$) were calculated using the following equation and the data obtained given in the same Table 1. It can be seen from Table 1 that, the addition of inhibitor to the aggressive solution reduces the corrosion rate of mild steel. The corrosion rate decreased and inhibition efficiency increased with increasing inhibitor concentration suggests that the inhibitor molecule act by adsorption on the metal surface [14,18].

Table 1: Inhibition efficiency of various concentrations of 5BI for corrosion of MS in 1M HCl obtained by weight loss measurements at 303K.

mediums	Concentration (M)	C_R ($\text{mg cm}^{-2} \text{h}^{-1}$)	η_w (%)	Θ
Blank	1.0	1.135	-	-
5BI	5.10^{-3}	0.0871	92.32	0.9021
	1.10^{-3}	0.1393	87.73	0.8773
	5.10^{-4}	0.1964	82.69	0.8269
	1.10^{-4}	0.2453	78.39	0.7839

Polarization potentiodynamic results

The polarization curves of mild steel in HCl medium in the presence and absence of inhibitor are shown in Fig. 2. It is illustrated that as the concentration increases there is a shift in the corrosion rates to lower values and inhibition efficiencies to upper quantities due to the act of inhibitor. Electrochemical corrosion kinetics parameters such as corrosion potential (E_{corr}), cathodic Tafel slope (β_c), the inhibition efficiency ($IE\%$) and corrosion current density (i_{corr}) were given in Table 2.

Figure 2. Polarisation curves of MS in 1 M HCl for various concentrations of 5BI at 303K.


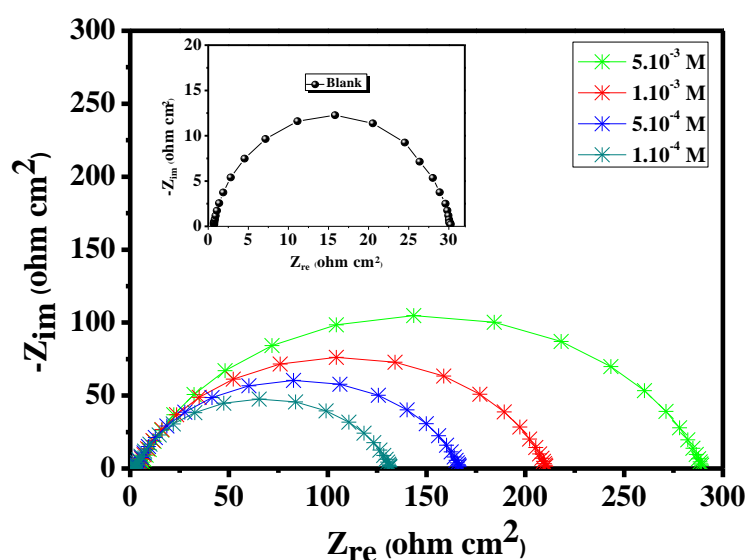
Analysis on the polarization curves show that in the presence of the inhibitor, the cathodic and anodic curves were slightly shifted. An inhibitor can be classified as cathodic or anodic type if the displacement in corrosion potential is more than 85 mV with respect to corrosion potential of the blank[1,5]. This indicates that 5BI acts as a mixed type inhibitor. As it would be expected both anodic and cathodic reactions of MS corrosion in hydrochloric acid solution were effectively suppressed, and this inhibition effect became more pronounced with increasing 5BI concentration. It is known that when the E_{corr} shifts slightly, the inhibitor act as mixed type inhibitor[5,6]. In addition, cathodic current-potential curves give rise to parallel Tafel lines, which indicates that the addition of the 5BI does not modify the mechanism of the reaction[3]. The results demonstrate that the inhibition efficiency increases with inhibitor concentration. The polarisation curves study also confirms the inhibiting character of 5BI obtained with weight loss measurements, however, $IE\%$ values determined using polarisation curves were smaller than those obtained by weight loss measurements. This difference was probably caused by the shorter immersion time in the case of polarisation curve measurements.

Table 2. Corrosion parameters for corrosion of MS with selected concentrations of 5BI in 1M HCl by Potentiodynamic polarization method at 303K.

Inhibitor	Concentration (M)	$-E_{corr}$ (mV/SCE)	$-\beta_c$ (mV dec ⁻¹)	i_{corr} ($\mu\text{A cm}^{-2}$)	η_{Tafel} (%)	θ
Blank	-	496	162.0	564.0	-	-
5BI	5.10^{-3}	485	155.4	55.21	90.21	0.9021
	1.10^{-3}	478	147.3	78.09	86.15	0.8615
	5.10^{-4}	483	154.2	103.7	81.61	0.8161
	1.10^{-4}	486	169.5	139.9	75.19	0.7519

Electrochemical impedance spectroscopy

Fig. 3 show the representative Nyquist plots of mild steel obtained in 1.0 M HCl solution in the absence and presence of various concentrations of 5BI. It is apparent from Fig. 3 that, the Nyquist plots of mild steel show a depressed semicircular shape and only one time constant was observed. This observation indicates that the corrosion of mild steel in 1.0 M HCl solution is mainly controlled by a charge transfer process[5,6]. Although the appearance of Nyquist plots remained the same, their diameter increased after the addition of organic compound to the corrosive solution. This increase was more and more pronounced with increasing inhibitor concentration, which indicates the adsorption of inhibitor molecules on the metal surface.

Figure 3. Nyquist curves for mild steel in 1 M HCl for selected concentrations of 5BI at 303K.


As it can be seen from Fig. 3, the Nyquist plots do not yield perfect semicircles as expected from the theory of *EIS*. The deviation from ideal semicircle is generally attributed to the frequency dispersion as well as to the inhomogeneities of surface and mass transport resistant[5,21]. The impedance spectra were fitted (Fig. 4) to the $R_s(R_{ct}CPE)$ equivalent circuit. Where R_s is the solution resistance, R_{ct} denotes the charge-transfer resistance and *CPE* is constant phase element. The introduction of *CPE* into the circuit was necessitated to explain the depression of the capacitance semicircle, which corresponds to surface heterogeneity resulting from surface roughness, impurities, and adsorption of inhibitors[14,17,25]. The impedance of this element is frequency-dependent and can be calculated using the Eq. 5:

$$Z_{CPE} = \frac{1}{Q(j\omega)^n} \quad (5)$$

Where Q is the *CPE* constant (in $\Omega^{-1} S^n \text{ cm}^{-2}$), ω is the angular frequency (in rad s^{-1}), $j^2 = -1$ is the imaginary number and n is a *CPE* exponent which can be used as a gauge for the heterogeneity or roughness of the surface. In addition, the double layer capacitances, C_{dl} , for a circuit including a *CPE* were calculated by using the following Eq. 6[12]:

$$C_{dl} = (Q \cdot R_{ct}^{1-n})^{1/n} \quad (6)$$

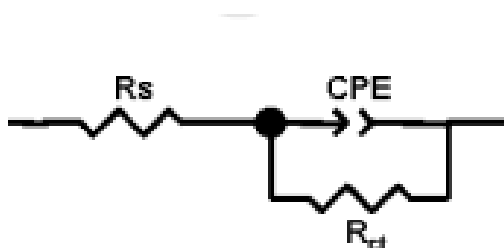
The R_{ct} values increase with the increase in concentration of indole derivative, indicating the formation of an insulated adsorption layer. Indeed, the inhibition efficiencies of this inhibitor, as will be seen, were evaluated by R_{ct} and C_{dl} values of the impedance. The more densely packed the monolayer of the inhibitor, the larger the diameter of the semicircle, which results in higher R_{ct} and lower C_{dl} values[4,5,16,20].

Table 3. AC-impedance parameters for corrosion of mild steel for selected concentrations of 5BI in 1M HCl at 303K.

Inhibitor	Concentration (M)	R_{ct} ($\Omega \text{ cm}^2$)	n	$Q \times 10^{-4}$ ($\text{s}^n \Omega^{-1} \text{cm}^{-2}$)	C_{dl} ($\mu\text{F cm}^{-2}$)	η_{EIS} (%)	θ
Blank	1.0	29.35	0.910	1.7610	91.6	-	-
5BI	5.10^{-3}	285.0	0.902	0.2881	17.09	89.70	0.8970
	1.10^{-3}	207.3	0.886	0.4712	25.97	85.84	0.8584
	5.10^{-4}	164.1	0.838	0.7699	33.06	82.11	0.8211
	1.10^{-4}	129.6	0.899	0.7378	43.75	77.35	0.7735

Data presented in Table 3 showed that, in all cases, the values of R_{ct} increase with increase in inhibitor concentration, while those of C_{dl} (derived, as will be discussed from CPE) tend to decrease. The decrease in C_{dl} is due to the gradual replacement of water molecules by the adsorption of the indole derivative at mild steel/1.0 M HCl solution interface, leading to a protective film on the steel surface, and then decreasing the extent of dissolution reaction[33].

Figure 4. Equivalent electrical circuit model.



Adsorption isotherm

The adsorption of the inhibitors at metal/solution interfaces can markedly change the corrosion resisting properties of metals. The efficiency of organic molecules as good corrosion inhibitors mainly depends on their adsorption ability on the metal surface. So, the investigation of the relation between corrosion inhibition and adsorption is of great importance[34,35]. In 1 M HCl, 5BI adsorption follows the Langmuir isotherm (Fig. 5) as per Eq.7[36]:

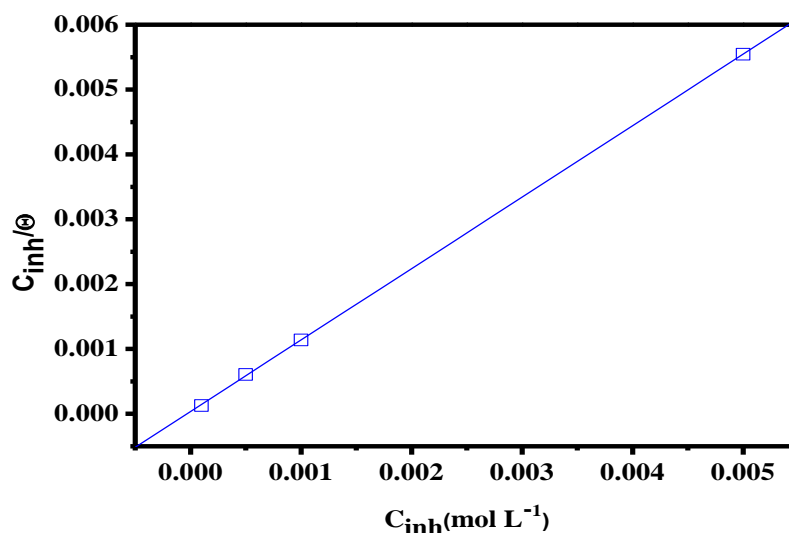
$$\frac{C}{\theta} = \frac{1}{K_{ads}} + C \quad (7)$$

Where, C is the concentration of the inhibitor, K_{ads} is the equilibrium constant of adsorption and θ is the surface coverage. The Langmuir approach is based on a molecular kinetic model of the adsorption-desorption process. On the other hand, the adsorption equilibrium constant (K_{ads}) is related to the standard free energy of adsorption (ΔG°_{ads}) of the inhibitor molecules by the following Eq. 8[35]:

$$K_{ads} = \frac{1}{55.5} \exp\left(\frac{-\Delta G^{\circ}_{ads}}{RT}\right) \quad (8)$$

Where R is the universal gas constant, T the absolute temperature in K , and 55.5 represents the molar concentration of water in the solution. Fig. 5 shows the plots of C_{inh}/θ versus C_{inh} and the expected linear relationship is obtained, and correlation coefficient is higher than 0.9999 . The value of K_{ads} was calculated as 27922 M^{-1} for 5BI at 303 K . The high value of the adsorption equilibrium constants reflect the high adsorption ability of this inhibitor on MS surface[2].

Figure 5: Langmuir adsorption of inhibitor on the MS surface in 1.0 M HCl solution at 303 K .



Molecular dynamic (Monte Carlo) simulation

The molecular dynamic simulations was performed to study the adsorption behaviour of the studied inhibitor (5BI) on the Fe (1 1 0) surface. In this simulation, Fe (1 1 0) surface was chosen among the three kinds of Fe surfaces (1 1 0, 1 0 0, 1 1 1), because Fe (1 1 0) surface is densely packed and is the most stable form[30,37]. The equilibrium configuration of simulated system is shown in Figure 6. From this figure, the 5BI molecules have a nearly flat orientation with respect to the iron surface, and it is evident that the presence of unoccupied d-orbital exhibits a tendency to obtain electrons from the adsorbed molecule. 5BI studied in this work has a number of lone pairs of electrons on atoms like N and O as well as electron clouds on the benzene ring. This will make it possible to provide electrons to the unoccupied orbitals of iron surface to form a stable coordination bonds. Figure 6 reveals that the studied inhibitor can be adsorbed on the Fe surface through the benzene ring and heteroatoms. As can be seen from Table 4, 5BI molecule showed the maximum adsorption energy ($-132.236 \text{ Kcal/mol}$) found during the simulation process which indicates that this molecule has the highest inhibition efficiency, which is in agreement with the experimental observations[29,30]

Figure 6. The most stable low energy configuration for the adsorption of the inhibitor on Fe (1 1 0) surface obtained through the Monte Carlo simulation.(a) side view, (b) top view.

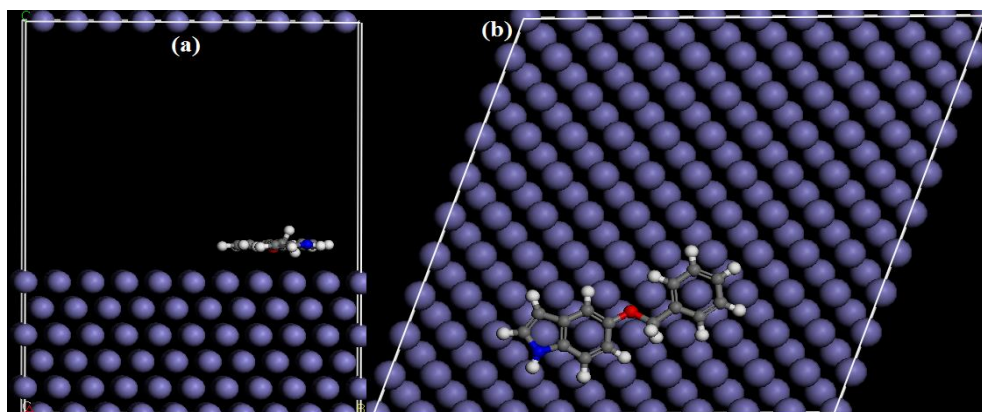


Table 4. Outputs and descriptors calculated by the Monte Carlo simulation for the lowest adsorption. Configurations of 5BI Fe (110) surface (in kcal/mol).

System	Total energy	Adsorption energy	Rigid adsorption energy	Deformation energy	dE _{ad} /dN _i inhibitor
Fe (1 1 0)/5BI	26.522	-132.236	-132.855	0.6186	-132.236

CONCLUSION

The 5BI have been investigated for their inhibition performance on mild steel corrosion in 1M HCl solution. The results of both gravimetric and electrochemical experiments showed that the compound inhibit mild steel corrosion in 1M HCl solution and the inhibition efficiency increases with increasing concentration of the inhibitor. The adsorption of studied 5BI obeys the Langmuir isotherm and involves competitive physisorption and chemisorption modes. Potentiodynamic polarization studies showed that the compound inhibit both anodic and cathodic half reactions associated with corrosion process. The *EIS* measurements showed that the compounds adsorb on mild steel surface to form protective film with essentially capacitive behavior. Monte Carlo simulations study showed that the 5BI adsorbed on the Fe (1 1 0) surface in a near flat orientation and the value of adsorption energy of the equilibrium configuration support the experimental inhibition efficiency of the compound.

ACKNOWLEDGEMENTS

Financial support from the Spanish Ministry of Science and Innovation (CTQ2010-61830) is gratefully acknowledged. The support given through a "INCRECYT" research contract to M. Zougagh.

REFERENCES

- [1] Yadav M, Gope L, Kumari N, Yadav P. *J Mol Liq* 2016;216:78–86. doi:10.1016/j.molliq.2015.12.106.
- [2] Yadav M, Sinha RR, Sarkar TK, Bahadur I, Ebenso EE. *J Mol Liq* 2015;212:686–98. doi:10.1016/j.molliq.2015.09.047.
- [3] Yadav M, Sinha RR, Kumar S, Bahadur I, Ebenso EE. *J Mol Liq* 2015;208:322–32. doi:10.1016/j.molliq.2015.05.005.
- [4] Yadav M, Kumar S, Sinha RR, Bahadur I, Ebenso EE. *J Mol Liq* 2015;211:135–45. doi:10.1016/j.molliq.2015.06.063.
- [5] Verma C, Quraishi MA, Singh A. *J Mol Liq* 2015;212:804–12. doi:10.1016/j.molliq.2015.10.026.
- [6] Verma C, Ebenso EE, Bahadur I, Obot IB, Quraishi MA. *J Mol Liq* 2015;212:209–18. doi:10.1016/j.molliq.2015.09.009.
- [7] Adardour L, Larouj M, Lgaz H, Belkhaouda M, Salghi R, Jodeh S, et al. *Pharma Chem* 2016;8:152–60.
- [8] Adardour L, Lgaz H, Salghi R, Larouj M, Jodeh S, Zougagh M, et al. *Pharm Lett* 2016;8:212–24.
- [9] Adardour L, Lgaz H, Salghi R, Larouj M, Jodeh S, Zougagh M, et al. *Pharm Lett* 2016;8:173–85.
- [10] Adardour L, Lgaz H, Salghi R, Larouj M, Jodeh S, Zougagh M, et al. *Pharm Lett* 2016;8:126–37.
- [11] Afia L, Larouj M, Lgaz H, Salghi R, Jodeh S, Samhan S, et al. *Pharma Chem* 2016;8:22–35.
- [12] Afia L, Larouj M, Salghi R, Jodeh S, Zougagh M, Rasem Hasan A, et al. *Pharma Chem* 2016;8:166–79.
- [13] Bousskri A, Salghi R, Anejjar A, Jodeh S, Quraishi MA, Larouj M, et al. *Pharma Chem* 2016;8:67–83.
- [14] El Makrini B, Larouj M, Lgaz H, Salghi R, Salman A, Belkhaouda M, et al. *Pharma Chem* 2016;8:227–37.
- [15] El Makrini B, Lgaz H, Larouj M, Salghi R, Rasem Hasan A, Belkhaouda M, et al. *Pharma Chem* 2016;8:256–68.
- [16] Larouj M, Belkhaouda M, Lgaz H, Salghi R, Jodeh S, Samhan S, et al. *Pharma Chem* 2016;8:114–33.
- [17] Larouj M, Lgaz H, Salghi R, Jodeh S, Messali M, Zougagh M, et al. *Mor J Chem* 2016;4:567–83.
- [18] Larouj M, Lgaz H, Salghi R, Oudda H, Jodeh S, Chetouani A. *Mor J Chem* 2016;4:425–36.
- [19] Larouj M, Lgaz H, Houda S, Zarrok H, Zarrouk A, Elmidaoui A, et al. *J Mater Environ Sci* 2015;6:3251–67.
- [20] Lgaz H, Anejjar A, Salghi R, Jodeh S, Zougagh M, Warad I, et al. *Int J Corros Scale Inhib* 2016;5:209–231.
- [21] Lgaz H, Benali O, Salghi R, Jodeh S, Larouj M, Hamed O, et al. *Pharma Chem* 2016;8:172–90.
- [22] Lgaz H, ELaoufir Y, Ramli Y, Larouj M, Zarrok H, Salghi R, et al. *Pharma Chem* 2015;7:36–45.
- [23] Lgaz H, Salghi R, Larouj M, Elfaydy M, Jodeh S, About H, et al. *Mor J Chem* 2016;4:592–612.

- [24] Lgaz H, Belkhaouda M, Larouj M, Salghi R, Jodeh S, Warad I, et al. *Mor J Chem* 2016;4:101–11.
- [25] Saadouni M, Larouj M, Salghi R, Lgaz H, Jodeh S, Zougagh M, et al. *Pharm Lett* 2016;8:96–107.
- [26] Saadouni M, Larouj M, Salghi R, Lgaz H, Jodeh S, Zougagh M, et al. *Pharm Lett* 2016;8:65–76.
- [27] Lotfi N, Lgaz H, Belkhaouda M, Larouj M, Salghi R, Jodeh S, et al. *Arab J Chem Environ Res* 2015;1:13–23.
- [28] *Materials Studio. Revision 6.0. Accelrys Inc., San Diego, USA; 2013.*
- [29] Eivani AR, Zhou J, Duszczky J. *Comput Mater Sci* 2012;54:370–7. doi:10.1016/j.commatsci.2011.10.016.
- [30] Verma C, Ebenso EE, Bahadur I, Obot IB, Quraishi MA. *J Mol Liq* 2015;212:209–18. doi:10.1016/j.molliq.2015.09.009.
- [31] Shahraki M, Dehdab M, Elmi S. *J Taiwan Inst Chem Eng* 2016.
- [32] Sasikumar Y, Adekunle AS, Olasunkanmi LO, Bahadur I, Baskar R, Kabanda MM, et al. *J Mol Liq* 2015;211:105–18. doi:10.1016/j.molliq.2015.06.052.
- [33] Kesavan D, Parameswari K, Lavanya M, Beatrice V, Ayyannan G, Sulochana N. *Chem Sci Rev Lett* 2014;2:415–22.
- [34] Yüce AO, Mert BD, Kardaş G, Yazıcı B. *Corros Sci* 2014;83:310–6.
- [35] Solmaz R. *Corros Sci* 2014;81:75–84.
- [36] Bentiss F, Lebrini M, Lagrenée M. *Corros Sci* 2005;47:2915–31.
- [37] Khaled KF, El-Maghraby A. *Arab J Chem* 2014;7:319–26. doi:10.1016/j.arabjc.2010.11.005.